201227014B

厚生労働科学研究費補助金

肝炎等克服緊急対策研究事業

小胞輸送ESCRT経路を利用したC型肝炎ウイルス排除

平成22年度－平成24年度

総合研究報告書

研究代表者　玉井恵一

平成25年 3 月

厚生労働科学研究費補助金

肝炎等克服緊急対策研究事業

小胞輸送 ESCRT 経路を利用したＣ型肝炎ウイルス排除

総合研究報告書

研究代表者　玉井恵一

平成 25 年 3 月

目次

小胞輸送 ESCRT 経路を利用した C 型肝炎ウイルス排除

研究報告者　玉井恵一 *　　研究分担者　菅村和夫 †　　研究分担者　田中伸幸 *

2013 年 3 月

1　概要

近年 HCV 培養系の確立によりライフサイクルの検討が行われている。我々は小胞輸送経路 ESCRT 分子である Hrs のノックアウト樹状細胞から産生されるエクソゾーム量が低下することを見いだした。エクソゾーム分泌とウイルス動態は酷似していることから、ESCRT 経路と HCV との関係を解析した。ESCRT 構成分子の機能低下 Huh7 細胞を樹立し、JFH1 を感染させたところ、上清中の JFH1-RNA はいずれの機能低下細胞においも最大約 1/50 に減少した。ESCRT 経路は JFH1 出芽に必要であることが示唆された。現在さらに、ヒト化肝臓マウスを用いて、in vivo における ESCRT 経路の役割を検討中である。

2　背景

C 型慢性肝炎は、C 型肝炎ウイルス（HCV）を原因とする疾患であり、国内では約 200 万人が罹患しているとされている。HCV を排除する治療としてペグインターフェロン・リバビリン併用療法が施行されているが、未だ難治性の患者が存在する。HCV に対する抗ウイルス薬としては、現在使用されているリバビリンの他、複数の薬剤が臨床試験中であるが、著明な効果の認められる薬剤はまだ報告されていない。HCV を標的とした抗ウイルス薬はプロテアーゼインヒビターやポリメラーゼインヒビター等、非構造タンパクを標的とした薬剤が主流であるが、HCV の細胞内ライフサイクルに着目した阻害剤はまだ報告がない。

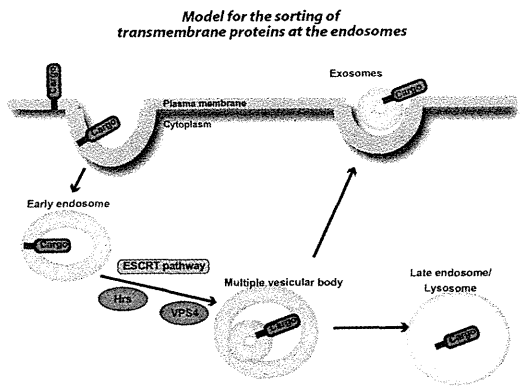

図 1　ESCRT 経路

これまで、HCV は培養系の確立が困難であったことから、そのライフサイクル・細胞内動態は不明な点が多かった。2005 年に in vitro で感染・再感染可能な HCV 株 JFH-1 が報告されてから [1]、HCV の細胞内動態の研究が可能になった。HCV はレセプターを介して細胞内にエンドサイトーシスされた後に、脱核・RNA 複製・翻訳・プロセッシングを経てウイルス粒子が構築され、細胞外に放出される。ウイルスが構築される際にはエンドソーム上に集められた構造タンパクがエンドソーム内に出芽することで粒子を形成すると考えられているが、その詳細な機構は依然不明である（図 1）。

我々は、以前からレセプターのエンドサイトーシス経路に関して報告してきた [2][3]。Epidermal growth factor (EGF) レセプターは、クラスリン依存性にエンドサイトーシスされたあと、EGF レセプターを含むエンドソームが ESCRT（Endosomal Sorting Complex Required for Transport）経路を

* 宮城県立がんセンター研究所　がん先進治療開発研究部
[tamaikeiichi@med.tohoku.ac.jp]
† 宮城県立がんセンター研究所　発がん制御研究部

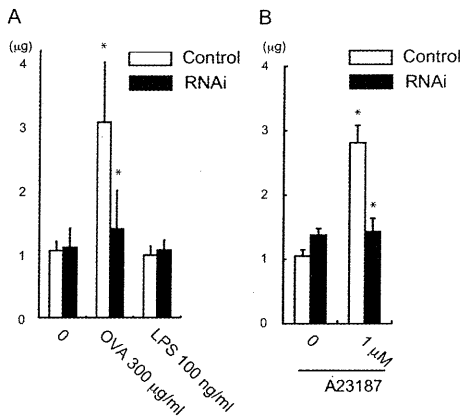

図 2 Hrs はエクソゾーム放出に必須である

経て multivesicular body（MVB）へと成熟した後に、リソソームでの分解を受ける。近年、MVB から内部の小胞をエクソゾームとして放出する機構が知られるようになった。エクソゾームは直径 50-100 nm の微小小胞であり、B 細胞や樹状細胞から放出され、MHC classII 等を含み免疫反応に関わるとされているが [5]、近年は mRNA や microRNA を含んで細胞間で情報の受け渡しをするなど広い生理学的作用が知られている [9]。我々は最近、このエクソゾームの放出には ESCRT 経路の最上流で機能する Hrs が必要であることを報告した [6]（図 2）。エクソゾームは HCV エンベロープを含み、C 型慢性肝炎の患者血清から分離されたエクソゾームから HCV RNA が検出されたとの報告がある [4]。我々は、エクソゾームの放出機構は HCV のアセンブリおよび出芽に酷似していることに着目し、小胞輸送経路 ESCRT と HCV の関連を探索した。

3 材料と方法

3.1 供試した細胞と調整

Huh7 細胞は 10 %仔ウシ血清を含む Dulbecco's Modified Eagle 培地で培養した。Huh7 を Hrs 特異的にノックダウンするために、Hrs 特異的な shRNA を発現するレトロウイルスベクターをトランスフェクションしたあと、2 μg/mL のピューロマイシンを用いて選択した。VPS4B 野生型・ドミナントネガティブ（E235Q）（Dr. Sundquist より供与）は、1 日目に FuGene6 (Roche) を用いてトランスフェクションし、2 日目に JFH1 を感染させて使用した（MOI = 0.01）。

3.2 Real-time PCR

HCV-RNA の定量は、以前に報告されているプライマーを用いて real-time PCR を用いて行った [8]。

3.3 エクソゾームの分離精製

培養上清中のエクソゾームを定量するために、10 cm シャーレに培養した細胞に 1 mM の A23187 (Ca ionophore, Sigma) を用いて刺激し、48 時間後に上清を回収した。培養上清に含まれるエクソゾームは、既報の手技を用いて精製した [6]。

3.4 ショ糖密度勾配

ショ糖密度勾配はショ糖を Hepes 緩衝液に溶解し（10% および 60%）、遠心管に 2 相に重層し、3 時間水平に倒した後に使用した。精製したエクソゾームを加え、100,000 g で 20 時間遠心して分画を作成した [7]。

3.5 ヒト化肝臓マウスの作成

実験動物中央研究所から TK-NOG マウスを購入し、ガンシクロビルを腹腔注射して肝障害を誘導したあと、ヒト正常肝細胞（Lonza 社）を一匹あたり $3x10^6$ を静注した。肝障害の誘導は血清 ALT を測定して検討した。マウス血清中のヒトアルブミン量を ELISA（Bethyl Laboratories）で測定し、肝のヒト化を確認した。

4 結果

4.1 Hrs ノックダウン Huh7 細胞の樹立

Hrs に対する shRNA 発現レトロウイルスベクターを導入した Huh7 細胞はウェスタンブロットを用いて Hrs 特異的にノックアウトされていることを確認した。ノックダウン細胞およびコントロール細胞を Ca ionophore で刺激した後に上清のエクソゾームを回収し、ショ糖密度勾配にかけたところ、既報と同様のフラクションに存在することを確認し（図 3）、電子顕微鏡による観察でも両者に形態学的な差はないことが確認された。

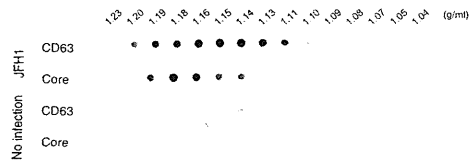

図 3 培養上清中の HCV とエクソゾームのショ糖密度勾配による分離

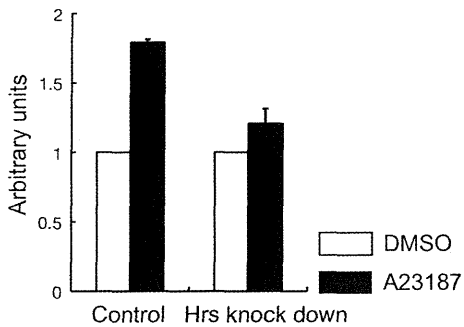

図 4 Hrs はエクソゾーム放出に影響する

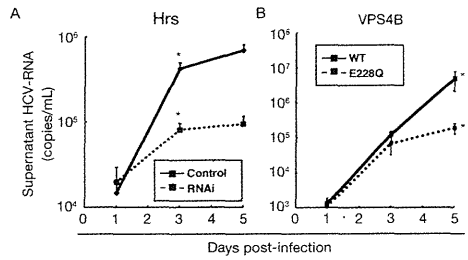

図 5 培養上清中の HCV-RNA 定量

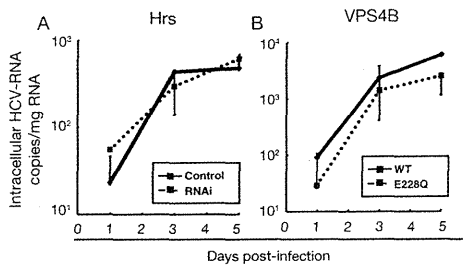

図 6 細胞内の HCV-RNA 定量

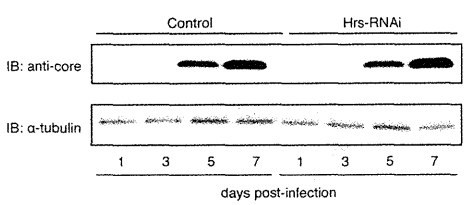

図 7 細胞内コア抗原の定量

4.2 Hrs はエクソゾーム放出に影響する

これらの細胞を使って、Ca ionophore で刺激し上清中に放出されたエクソゾームを定量して、Hrs がエクソゾーム放出に影響するかどうかを調べた。刺激後 48 時間の時点での上清中のエクソゾームは Hrs ノックダウン Huh7 細胞において著明に減少した（図 4）。

4.3 HCV コアタンパクはエクソゾームと同じ分画に存在する

Huh7 細胞に JFH-1 を感染させ、その上清を回収し、エクソゾームを分離精製し、ショ糖密度勾配で分画した。エクソゾームマーカー CD63 あるいは HCV コアタンパクで検出したところ、両者でみられるピークはほぼ同じ分画に存在した（図 3）。

4.4 ESCRT 機能不全細胞では、JFH1 の放出量が減少する。

Hrs ノックダウン Huh7 細胞に JFH1 を感染させ、上清に放出される HCV-RNA を経時的に real-timePCR で定量した。Hrs ノックダウン細胞では、コントロール細胞に比して約 2 log(10) の JFH1-RNA の減少を認めた（図 5）。同様の実験を VPS4B ドミナントネガティブ発現 Huh7 を用いて行ったが、同じ傾向を認めた。細胞内の JFH1-RNA 量は Hrs の有無あるいは VPS4B の有無で明らかな差を認めなかった（図 6）。また、細胞内の HCV コア抗原の量にも差はなかった（図 7）。

細胞の増殖能が HCV 放出量に影響する可能性を検討するために、Huh7 細胞に放射線（25Gy）を照射し、増殖を停止させた上で HCV の放出量を比較した。その結果、Hrs ノックダウン細胞では前の結果と同様に上清中の HCV-RNA 量が減少した（図 8）。

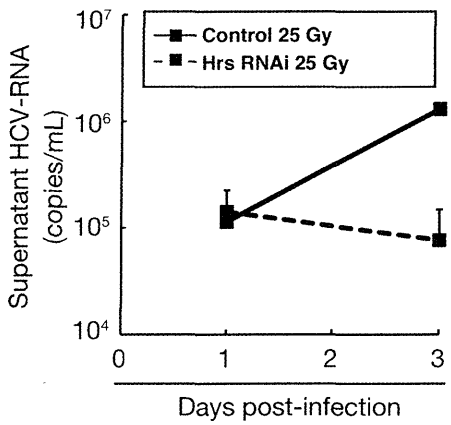

図 8 Hrs は放射線照射後の細胞においても HCV 放出量に影響する

4.5 ESCRT 機能不全細胞では、JFH1 の感染価が減少する

Hrs ノックダウン細胞において、JFH1 の感染性粒子の放出に対する影響を調べるために、培養上清中の ffu を測定した。その結果、Hrs ノックダウン細胞においては、感染性粒子の産生も減少していることが分かった（図 9）。

4.6 Hrs 肝特異的ノックアウトマウスは明らかな表現型を認めない

Hrs の肝における生理的意義を探索するために、肝特異的 Hrs ノックアウトマウスを作成した。その結果、意外なことにノックアウトマウスは、少なくとも通常の飼育状態では明らかな表現型を表さなかった。このことは、Hrs を含む ESCRT 経路が、肝においては HCV 感染状態のような病的な状態でのみ機能することを示唆しており、実際のヒト肝臓において ESCRT 経路をターゲットとすることは、副作用の少ない治療となることも期待でき、更なる検討が必要と考えられた。

4.7 In vivo における Hrs ノックダウンおよび HCV に対する影響

In vivo における解析を行うために、ヒト化肝臓マウスに JFH-1 を感染させ、アデノウイルスベクターを用いて Hrs ノックダウンを行い、血清中の JFH-1-RNA を測定した。アデノウイルスでノックダウンした個体では、コントロールと比べて JFH-1-RNA が減少した。現在個体数を増やして検討中である。

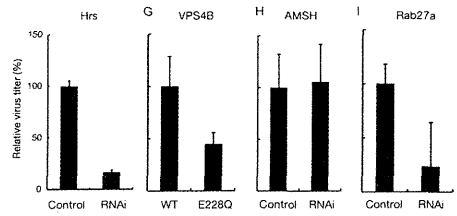

図 9 培養上清中の JFH-1 感染性粒子の量

5 考案

本研究では、Huh7 細胞を用いて、ESCRT 経路を阻害することで HCV 放出が抑制されることを示した。同時に Ca ionophore 刺激で放出されるエクソゾーム量も減少していた。エクソゾームには HCV が含まれるとされており [3]、本研究でも HCV とエクソゾームはショ糖密度勾配において同じ分画に存在することから、HCV とエクソゾームは同じ ESCRT 経路を介して放出されている可能性が考えられた。今後は免疫電子顕微鏡を用いて細胞内外の微小粒子を観察することで、より直接的にこの現象を示すことが必要である。

ESCRT 経路は MVB 形成に必須の経路であり、エクソゾームは MVB の内部小胞が放出されたものとされているが [6]、エクソゾームと MVB との関連性には議論が多い。エクソゾームの形成にはセラミドを必要とするが、ESCRT 経路には依存していなかったとの報告もある [7]。放出するエクソゾームの内容物によって依存する経路が違うことも予想され、今後詳細な検討が必要である。

本研究では、in vivo における ESCRT 経路の HCV に対する影響も検討した。その結果、まだ予備実験の段階ではあるが、Hrs ノックダウンによって HCV 放出が抑制されることが示唆された。肝特異的 Hrs ノックアウトマウスでは、現在までは肝に表現型を認めておらず、生理的な状態においては、肝における Hrs の機能は乏しく、HCV 感染時にお

いてはじめて機能する可能性が示唆された。従って、肝における Hrs をヒトでコントロールすることは、副作用の点からは望ましいと考えられた。

本研究からは、エクソゾーム経路を利用して HCV が放出されている可能性が示唆された。また、in vivo においても、この現象が再現される可能性を見いだした。本研究は HCV ライフサイクルの一端を明らかにするものであり、この経路を阻害することが出来れば、新たな抗ウイルス薬の開発につながるものと考えられる。

6 謝辞

本研究に協力頂いた、技術員　中村真央に感謝する。

7 研究発表

7.1 論文発表

1. T. Imai, K. Tamai, S. Oizumi, K. Oyama, K. Yamaguchi, I. Sato, K. Satoh, K. Matsuura, S. Saijo, K. Sugamura, N. Tanaka, CD271 defines a stem cell-like population in hypopharyngeal cancer, PLoS One 8 (2013) e62002.
2. K. Tamai, M. Shiina, N. Tanaka, T. Nakano, A. Yamamoto, Y. Kondo, E. Kakazu, J. Inoue, K. Fukushima, K. Sano, Y. Ueno, T. Shimosegawa, K. Sugamura, Regulation of hepatitis C virus secretion by the Hrs-dependent exosomal pathway, Virology 422 (2012) 377-385.
3. Y. Kondo, Y. Ueno, M. Ninomiya, K. Tamai, Y. Tanaka, J. Inoue, E. Kakazu, K. Kobayashi, O. Kimura, M. Miura, T. Yamamoto, T. Kobayashi, T. Igarashi, T. Shimosegawa, Sequential immunological analysis of HBV/HCV co-infected patients during Peg-IFN/RBV therapy, J Gastroenterol 47 (2012) 1323-1335.
4. Y. Kondo, Y. Ueno, M. Ninomiya, K. Tamai, Y. Tanaka, J. Inoue, E. Kakazu, K. Kobayashi, O. Kimura, M. Miura, T. Yamamoto, T. Kobayashi, T. Igarashi, T. Shimosegawa, Sequential immunological analysis of HBV/HCV co-infected patients during Peg-IFN/RBV therapy, J Gastroenterol (2012).
5. Y. Amano, Y. Yamashita, K. Kojima, K. Yoshino, N. Tanaka, K. Sugamura, T. Takeshita, Hrs recognizes a hydrophobic amino acid cluster in cytokine receptors during ubiquitin-independent endosomal sorting, J Biol Chem 286 (2011) 15458-15472.
6. S. Suzuki, K. Tamai, M. Watanabe, M. Kyuuma, M. Ono, K. Sugamura, N. Tanaka, AMSH is required to degrade ubiquitinated proteins in the central nervous system, Biochem Biophys Res Commun 408 (2011) 582-588.
7. Y. Kondo, Y. Ueno, E. Kakazu, K. Kobayashi, M. Shiina, K. Tamai, K. Machida, J. Inoue, Y. Wakui, K. Fukushima, N. Obara, O. Kimura, T. Shimosegawa, Lymphotropic HCV strain can infect human primary naive CD4+ cells and affect their proliferation and IFN-gamma secretion activity, J Gastroenterol 46 (2011) 232-241.
8. J. Inoue, Y. Ueno, Y. Wakui, H. Niitsuma, K. Fukushima, Y. Yamagiwa, M. Shiina, Y. Kondo, E. Kakazu, K. Tamai, N. Obara, T. Iwasaki, T. Shimosegawa, Four-year study of lamivudine and adefovir combination therapy in lamivudine-resistant hepatitis B patients: influence of hepatitis B virus genotype and resistance mutation pattern, J Viral Hepat 18 (2011) 206-215.
9. K. Tamai, N. Tanaka, T. Nakano, E. Kakazu, Y. Kondo, J. Inoue, M. Shiina, K. Fukushima, T. Hoshino, K. Sano, Y. Ueno, T. Shimosegawa, K. Sugamura, Exosome secretion of dendritic cells is regulated by Hrs,

an ESCRT-0 protein, Biochem Biophys Res Commun 399 (2010) 384-390.

10. N. Obara, K. Fukushima, Y. Ueno, Y. Wakui, O. Kimura, K. Tamai, E. Kakazu, J. Inoue, Y. Kondo, N. Ogawa, K. Sato, T. Tsuduki, K. Ishida, T. Shimosegawa, Possible involvement and the mechanisms of excess trans-fatty acid consumption in severe NAFLD in mice, J Hepatol 53 (2010) 326-334.
11. Y. Kondo, Y. Ueno, K. Kobayashi, E. Kakazu, M. Shiina, J. Inoue, K. Tamai, Y. Wakui, Y. Tanaka, M. Ninomiya, N. Obara, K. Fukushima, M. Ishii, T. Kobayashi, H. Niitsuma, S. Kon, T. Shimosegawa, Hepatitis B virus replication could enhance regulatory T cell activity by producing soluble heat shock protein 60 from hepatocytes, J Infect Dis 202 (2010) 202-213.

8 学会発表

1. 玉井恵一、菅村和夫、田中伸幸：CD274(-) 細胞分画は胆管癌細胞株においてがん幹細胞様の性質を有する. 第 99 回日本消化器病学会総会, 鹿児島, 2013.3
2. 玉井恵一、船木智、遠藤博之、山口壹範、佐藤賢一、菅村和夫、田中伸幸：CD274(-) 細胞分画は胆管癌細胞株においてがん幹細胞様の性質を有する。第 66 回日本細菌学会東北支部総会、仙台、2012.8
3. Tamai Keiichi, Funaki Tomo, Endo Hiroyuki, Yamaguchi Kazunori, Satoh Kennichi, Sugamura Kazuo, Tanaka Nobuyuki. Absence of CD274 accelerates cancer stem cell-phenotypes in cholangiocellular carcinoma cell lines. 71st Annual Meeting of the Japanese Cancer Association
4. 玉井恵一、田中伸幸、上野義之、下瀬川徹、菅村和夫：HCV 感染における小胞輸送タンパク Hrs の役割. 第 6 4 回日本細菌学会東北地方会, 仙台, 2010.8
5. 須賀淳子、 菅村和夫、田中伸幸：C-terminal region of ErbB3 controls ErbB2/ErbB3 heterodimer signaling through ubiquitin-dependent receptor degradation 第 69 回日本癌学会学術総会, 大阪, 2010.9
6. 玉井恵一、田中伸幸、上野義之、下瀬川徹、菅村和夫：Possible regulation of hepatitis C virus secretion by Hrs-dependent exosomal pathway 第 69 回日本癌学会学術総会, 大阪, 2010.9

9 知的財産権の出願・登録状況

9.1 特許取得

該当なし

9.2 実用新案登録

該当なし

9.3 その他

該当なし

参考文献

[1] T. Wakita, T. Pietschmann, T. Kato, T. Date, M. Miyamoto, Z. Zhao, K. Murthy, A. Habermann, H.G. Krausslich, M. Mizokami, R. Bartenschlager, T.J. Liang, Production of infectious hepatitis C virus in tissue culture from a cloned viral genome, Nat Med 11 (2005) 791-796.

[2] K. Tamai, M. Toyoshima, N. Tanaka, N. Yamamoto, Y. Owada, H. Kiyonari, K. Murata, Y. Ueno, M. Ono, T. Shimosegawa, N. Yaegashi, M. Watanabe, K. Sugamura, Loss of hrs in the central nervous system causes accumulation of ubiquitinated proteins and neurodegeneration, Am J Pathol 173 (2008) 1806-1817.

[3] K. Tamai, N. Tanaka, A. Nara, A. Yamamoto, I. Nakagawa, T. Yoshimori, Y.

Ueno, T. Shimosegawa, K. Sugamura, Role of Hrs in maturation of autophagosomes in mammalian cells, Biochem Biophys Res Commun 360 (2007) 721-727.

[4] F. Masciopinto, C. Giovani, S. Campagnoli, L. Galli-Stampino, P. Colombatto, M. Brunetto, T.S. Yen, M. Houghton, P. Pileri, S. Abrignani, Association of hepatitis C virus envelope proteins with exosomes, Eur J Immunol 34 (2004) 2834-2842.

[5] G. Raposo, H.W. Nijman, W. Stoorvogel, R. Liejendekker, C.V. Harding, C.J. Melief, H.J. Geuze, B lymphocytes secrete antigen-presenting vesicles, J Exp Med 183 (1996) 1161-1172.

[6] K. Tamai, N. Tanaka, T. Nakano, E. Kakazu, Y. Kondo, J. Inoue, M. Shiina, K. Fukushima, T. Hoshino, K. Sano, Y. Ueno, T. Shimosegawa, K. Sugamura, Exosome secretion of dendritic cells is regulated by Hrs, an ESCRT-0 protein, Biochem Biophys Res Commun 399 (2010) 384-390.

[7] S. Abe, E. Davies, Quantitative analysis of polysome profiles using a baseline from uncentrifuged blank gradients., Memories of the College of Agriculture, Ehime University 31 (1986) 187-199.

[8] M. Shiina, B. Rehermann, Cell culture-produced hepatitis C virus impairs plasmacytoid dendritic cell function, Hepatology 47 (2008) 385-395.

[9] S. Rana, M. Zoller, Exosome target cell selection and the importance of exosomal tetraspanins: a hypothesis, Biochem Soc Trans 39 (2011) 559-562.

10　研究成果の印刷物

Virology 422 (2012) 377–385

Contents lists available at SciVerse ScienceDirect

Virology

journal homepage: www.elsevier.com/locate/yviro

Regulation of hepatitis C virus secretion by the Hrs-dependent exosomal pathway

Keiichi Tamai [a,b], Masaaki Shiina [b], Nobuyuki Tanaka [a,d,*], Takashi Nakano [e], Akitsugu Yamamoto [f], Yasuteru Kondo [b], Eiji Kakazu [b], Jun Inoue [b], Koji Fukushima [b], Kouichi Sano [e], Yoshiyuki Ueno [b], Tooru Shimosegawa [b], Kazuo Sugamura [a,c]

[a] Division of Cancer Biology and Therapeutics, Miyagi Cancer Center Research Institute, Natori 981-1293, Japan
[b] Department of Gastroenterology, Tohoku University Graduate School of Medicine, Sendai, 980-8575, Japan
[c] Department of Microbiology and Immunology, Tohoku University Graduate School of Medicine, Sendai, 980-8575, Japan
[d] Department of Cancer Science, Tohoku University Graduate School of Medicine, Sendai, 980-8575, Japan
[e] Department of Microbiology and Infection Control, Faculty of Medicine, Osaka Medical College, Takatsuki, Osaka 569-8686, Japan
[f] Department of Animal Bio-Science, Faculty of Bio-Science, Nagahama Institute of Bio-Science and Technology, Nagahama, 526-0829, Japan

ARTICLE INFO

Article history:
Received 14 July 2011
Returned to author for revision
6 September 2011
Accepted 10 November 2011
Available online 3 December 2011

Keywords:
Hrs
ESCRT
HCV

ABSTRACT

The molecular mechanisms of assembly and budding of hepatitis C virus (HCV) remain poorly understood. The budding of several enveloped viruses requires an endosomal sorting complex required for transport (ESCRT), which is part of the cellular machinery used to form multivesicular bodies (MVBs). Here, we demonstrated that Hrs, an ESCRT-0 component, is critical for the budding of HCV through the exosomal secretion pathway. Hrs depletion caused reduced exosome production, which paralleled with the decrease of HCV replication in the host cell, and that in the culture supernatant. Sucrose-density gradient separation of the culture supernatant of HCV-infected cells revealed the co-existence of HCV core proteins and the exosome marker. Furthermore, both the core protein and an envelope protein of HCV were detected in the intraluminal vesicles of MVBs. These results suggested that HCV secretion from host cells requires Hrs-dependent exosomal pathway in which the viral assembly is also involved.

© 2011 Elsevier Inc. All rights reserved.

Introduction

Hepatitis C virus (HCV) is a major cause of chronic liver disease, with about 170 million people infected worldwide. It is important to identify the molecular basis of HCV infection, propagation, and pathogenesis in humans. HCV is a positive-strand RNA virus belonging to the *Flaviviridae* family and the sole member of the genus *Hepacivirus*. The HCV RNA genome serves as a template for viral replication and as a messenger RNA for viral production. It is translated into a single immature polyprotein of approximately ~3000 amino acids that is further cleaved into at least 10 mature proteins by proteases (Asselah et al., 2009).

The HCV life cycle starts with virion attachment, especially through its envelope glycoproteins E1 and E2, to specific receptors on the host cells, which include CD81, claudin-1, and the class B member I scavenger receptor (Evans et al., 2007; Murray et al., 2008). These receptors and co-receptors are also required for HCV entry, which involves an additional clathrin-mediated post-internalization step and delivery into early endosomes (Burlone and Budkowska, 2009). Recently, the complete replication of HCV in a cell culture system was achieved (Wakita et al., 2005). Nevertheless, little is known about how the assembled HCV virion is released from the cytoplasm.

Extensive research on human immunodeficiency virus (HIV) has shown that the ESCRT (endosomal sorting complex required for transport) machinery plays a crucial role in virion assembly and budding from cellular membranes: The late-domain (L-domain) motif of HIV-Gag binds TSG101 (an ESCRT-I component) and Alix (a protein that bridges ESCRT-I and ESCRT-III). Virion assembly, budding, and release are subsequently achieved with help from the sequential downstream ESCRT machinery (Chen and Lamb, 2008). Other enveloped viruses, such as hepatitis B virus and human T-cell leukemia virus type I, also hijack the cellular membrane trafficking and sorting networks to accumulate and assemble their viral components, after which the nascent virions pinch themselves off for release (Chen and Lamb, 2008).

Similar to an enveloped virus particle that buds from the host-cell surface, small vesicles, called exosomes, are physiologically secreted from a variety of cells (Denzer et al., 2000; van Niel et al., 2006). Exosomes are nanovesicles (60–90 nm in diameter) surrounded by a

Abbreviations: ER, endoplasmic reticulum; ESCRT, endosomal sorting complex required for transport; HCV, hepatitis C virus; HHV-6, human herpes virus-6; HIV, human immunodeficiency virus; ILV, intraluminal vesicle L-domain, late-domain; MVB, multivesicular body; shRNA, short hairpin RNA.

* Corresponding author at: Division of Cancer Biology and Therapeutics, Miyagi Cancer Center Research Institute, 47-1 Nodayama, Medeshima-Shiode, Natori, Miyagi, 981-1293, Japan. Fax: +81 22 381 1168.
E-mail address: tanaka@med.tohoku.ac.jp (N. Tanaka).

0042-6822/$ – see front matter © 2011 Elsevier Inc. All rights reserved.
doi:10.1016/j.virol.2011.11.009

of sorting, an AAA-type ATPase, VPS4, disrupts the ESCRT complexes, and the membrane with its accumulated cargo is invaginated into the maturing endosome to produce an MVB. A deficiency of Hrs results in abnormally enlarged endosomes and a marked reduction in cargo sorting to MVBs. The enlarged endosomes accumulate ligand-activated membrane-bound growth factor receptors (Tanaka et al., 2008). In this context, we recently demonstrated that Hrs is also required in dendritic cells for exosome secretion and antigen presentation via exosomes (Tamai et al., 2010).

Relationships are also reported between membrane trafficking and the HCV life cycle. ESCRT-III contributes to HCV release in Huh7 cells (Ariumi et al., 2011; Corless et al., 2010), as does transfection of these cells with RNAi against Atg7, an essential autophagy gene (Tanida et al., 2009). Another study suggested that human plasma contains exosomes and that in HCV patients, viral RNA is associated with these circulating vesicle (Masciopinto et al., 2004). Since Hrs, an ESCRT-0 component, is involved in the autophagic pathway (Tamai et al., 2007) and required for exosome secretion, we hypothesized that Hrs plays a role in the HCV life cycle. Here we demonstrated that the Hrs-dependent exosomal pathway plays an important role in HCV release.

Results

HCV core protein localizes to exosome-rich fractions

A relationship between virus production and the exosome pathway has been suggested for HIV and human herpes virus 6 (HHV6) (Lenassi et al.; Mori et al., 2008). We suspected that HCV also utilizes the exosome pathway for its release from host cells. To examine this possibility, we subjected the culture supernatants of HCV JFH-1-infected Huh7 cells to sucrose density gradient centrifugation and analyzed the fractions for exosomes and HCV. Interestingly, the identical fractions were positive both for the exosome marker CD63 and for the HCV core protein (Fig. 1A). Notably, more CD63-positive exosomes were found in the HCV-infected Huh7 cells than in uninfected cells. To exclude a possibility that the cytopathic effect (CPE) induced by the infection of JFH-1 affects the amount of CD63 in the supernatant, we monitored the CPE by the lactate dehydrogenase (LDH) assay. In Huh7 cells, we observed slight increase of LDH at post-infection day 5 (Fig. 1B). As a positive control, we also investigated the CPE in Huh7.5.1, which is more susceptible to JFH-1 infection. LDH level was approximately two-times higher in this Huh7.5.1 cells than the non-infected, which is compatible with a previous report (Shiina and Rehermann, 2008). Purified exosomes from the culture supernatant of JFH-1-infected Huh7 cells possessed HCV-infectivity to Huh7 cells (Fig. 1C). These results indicated that the exosome secretion was mainly activated during HCV infection.

We next addressed whether HCV localizes to the intraluminal vesicles within the MVBs of JFH-1-infected Huh7 cells. Using confocal microscopy, we found that N-Rh-PE-positive dots (an exosome and MVB marker) were likely to colocalize with HCV-core-positive dots (Fig. 1D, upper panels). As a negative control, immunofluorescence staining was performed with anti-HCV-core and mitochondrial marker (Mitotracker (Molecular Probes)), which reportedly do not colocalize with each other (Lai et al., 2010). We did observe that HCV-core protein was not colocalized to mitochondria (Fig. 1D, lower panels). By immunoelectron microscopy, we detected positive immunogold staining for the HCV core antigen on the intraluminal vesicles (Fig. 1E). Similarly, positive immunogold staining for the HCV envelope protein E2 was observed on intraluminal vesicles within MVBs (Fig. 1F). To make the relationships between HCV particles and exosomes clearer, we performed the double-staining of immunoelectron microscopy using anti-CD63 and anti-core protein. We observed the colocalization of CD63 and HCV-core in the intraluminal vesicles in the MVB (Fig. 1G). These data together suggested that HCV virions and exosomes are present in the same or very similar compartments.

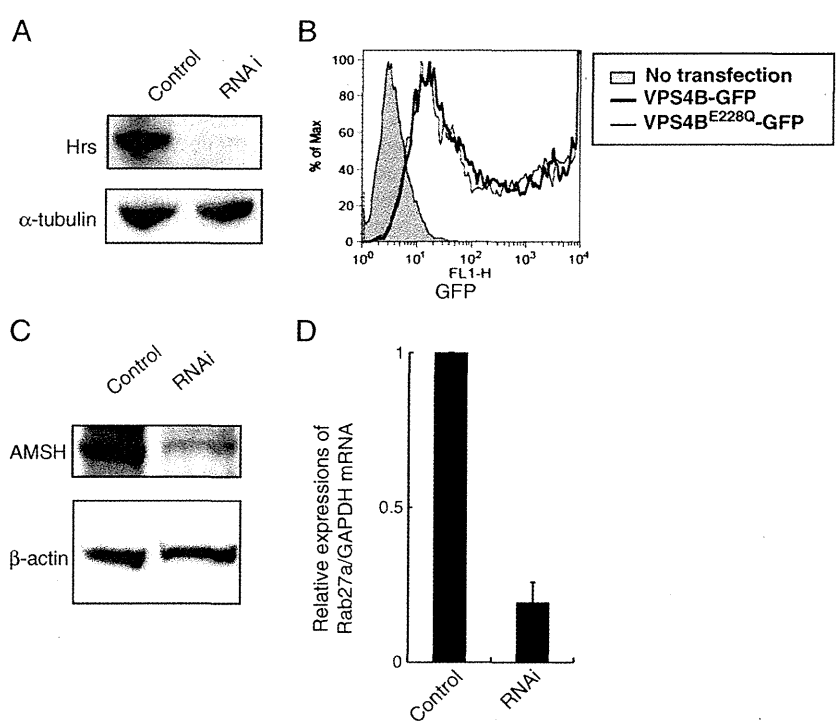

Fig. 2. Establishment of Huh7 lines with knocked-down Hrs, AMSH or Rab27a, and overexpressed VPS4B. (A) Western blot analysis of total-cell lysates from control and Hrs (A) and AMSH (C) knock-down Huh7 cells. (B) Flow-cytometry analysis of Huh7 cells overexpressing GFP-fused VPS4B (wild-type and dominant-negative (E228Q) forms). (D) Quantitative real-time PCR analysis of Rab27a in Huh7 cells. Rab27a mRNA expression was normalized to GAPDH.

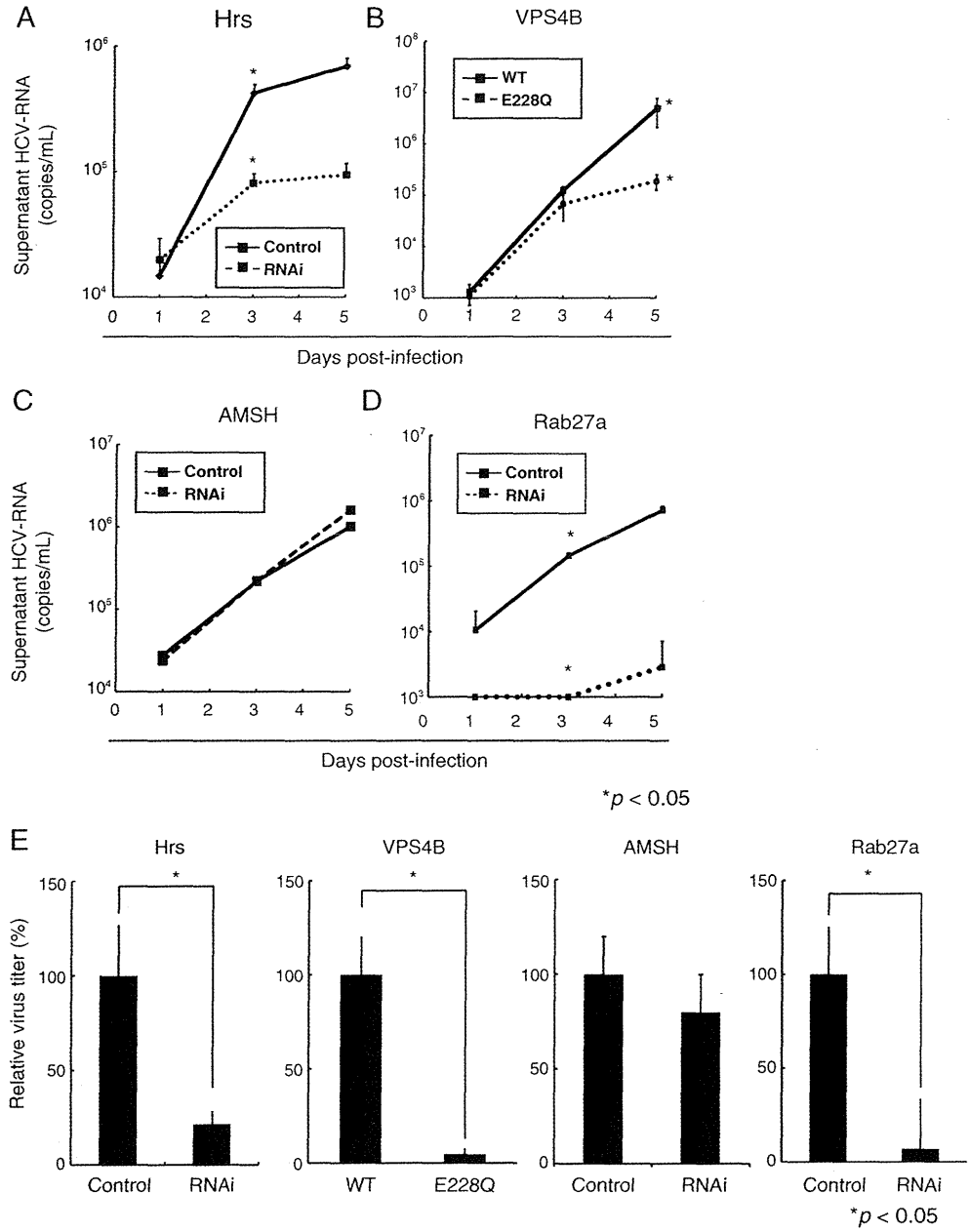

Fig. 4. Hrs, VPS4B, and Rab27a, but not AMSH, affect HCV release. (A to D) HCV-RNA in the culture supernatant on the indicated day after infection, measured using real-time PCR. Huh7 cells were infected with HCV (MOI = 0.01). (E) Infectious HCV particles in the supernatant were measured by a focus-forming unit assay at day 5 post-infection.

2010). Although the detailed mechanisms are not fully elucidated, we propose that normal trafficking via MVBs is required for the formation of complete HCV particles.

In this study we found the relationship between HCV and exosome from three experiments. First, by using immunoelectron microscopy, we demonstrated that HCV core protein and CD63 colocalized each other in MVB. Second, the confocal microscopy analyses revealed that exosomal marker N-Rh-PE colocalized with the core protein. Third, purified exosomal fraction possessed infectivity to Huh7 cells. These results suggest that HCV particles indeed colocalize with exosomes, and contain exosome marker proteins. This notion is not surprising because various viruses have been shown to acquire parts of host cell-derived proteins (Kolegraff et al., 2006). These phenomenons seem to reflect a fact that a number of virus carry host factors either during the assembly, or the release from their respective host cells. In Fig. 1A, the peaks for the HCV core protein and CD63 do not entirely correspond (1.18 g/ml and 1.15 g/ml, respectively). In general, HCV particles and exosomes in diameter are very similar (50 nm and 30–100 nm, respectively). On the other hand, HCV particles contain genomes which consist of a positive-sense RNA molecule approximately 9.6 kb in length. It is possible that the density of HCV particles is somewhat higher than that of exosomes. Further study will be required to elucidate how HCV particles and exosomes were similarly or differentially produced in MVB.

The detailed mechanisms by which HCV utilizes the ESCRT machinery for its release are still unknown. Capsid proteins of several viruses, such as HIV and HTLV-1 interact with ESCRT proteins via the

A previous study suggested that human herpes virus-6 (HHV-6) is released together with internal vesicles through MVBs by the cellular exosomal pathway: HHV-6 undergoes maturation in the trans-Golgi network (TGN) and post-TGN-derived vacuoles, which express an exosomal marker, CD63, and MVBs contain HHV-6 envelope glycoproteins along with CD63 (Mori et al., 2008). In addition, HIV virions released into the culture supernatant also contain CD63 (Gould et al., 2003), and CD63-positive exosomes derived from HIV-infected cells contain HIV Gag proteins (Booth et al., 2006). Here we showed that CD63-positive exosomal fractions can also contain HCV particles. Taken together, these observations support the idea that exosomal secretion and the budding of HCV, HHV6, and HIV share overlapping pathways.

Conclusion

Since we here provide evidence that Hrs is important in exosome secretion and HCV release, Hrs may be one of the key players in HCV release, through the exosomal pathway. Controlling this pathway could become one of novel therapeutic strategies for chronic viral infections.

Materials and methods

Ethics statements

This study was conducted according to the principles expressed in the Declaration of Helsinki. The study was approved by the research committees of the Miyagi Cancer Center and Tohoku University.

Cells

Huh7 and Huh7.5.1 (gift from Dr. Chisari, The Scripps Research Institute, CA) cells were maintained in Dulbecco's modified essential medium containing 10% fetal calf serum and antibiotics. To express Hrs-specific short hairpin RNA (shRNA), a retroviral vector was generated as described previously (Tamai et al., 2007). In brief, a sequence encoding human Hrs-specific shRNA, was inserted into pSIREN-RetroQ (BD Biosciences) to make pSIREN-RetroQ-Hrs. The target sequence consisted of nucleotides 302–320 (5′-AGGTAAACGTCCGTAACAA-3′) of the human hrs cDNA. A control plasmid, pSIREN-RetroQ-Luc, targeted bp 413–434 of firefly luciferase (5′-GCAATAGTTCACGCTGAAAAG-3′). The retrovirus was prepared as previously described (Tamai et al., 2007). A human AMSH-specific short hairpin RNA (shRNA), pSIREN-RetroQ-AMSH, was also generated using pSIREN-RetroQ (Kyuuma et al., 2007). The target sequence within the human AMSH cDNA was nucleotides 651–669 (5′-GCAGCAATTGGAACAGGAA-3′). A human Rab27a-specific shRNA lentiviral vector was purchased from Sigma. LDH assay was performed according to the manufacturer's protocol (Roche, Basel, Switzerland).

Isolation and purification of exosomes

Exosomes were purified as previously described (Ostrowski et al., 2010). In brief, the cell culture medium was centrifuged for 10 min at $300\times g$, 10 min at $1200\times g$, and 30 min at $10{,}000\times g$ to remove cells and debris. The supernatant obtained from the last spin was then centrifuged for 60 min at $100{,}000\times g$, and the pellet was solubilized in lysis buffer (1% Nonidet P-40, 20 mM Tris–HCl (pH 7.5), 150 mM NaCl, 1 mM EDTA, 1 mM phenylmethylsulfonyl fluoride, and 20 μg/ml aprotinin) and analyzed by BCA protein assay (Pierce, Rockford, IL, USA), according to the manufacturer's protocol. For sucrose density gradient centrifugation, sucrose gradients were prepared according to a former procedure (Abe and Davies, 1986). In brief, 5 ml 72% sucrose/PBS was overlaid with 5 ml 8.4% sucrose/PBS in 10 ml tubes, and the tubes stoppered and kept horizontal for 3 h at room temperature, after which they were slowly returned to the upright position. The exosomal suspension was layered onto a gradient sucrose and centrifuged at $100{,}000\times g$ for 20 h in a Beckmann SW41Ti rotor.

Western blotting

Immunoblotting was performed as described previously (Takeuchi et al., 1999). In brief, total cell lysates were prepared with NP-40-containing lysis buffer (described above). The lysates were pre-cleared by centrifugation ($10{,}000\times g$) for 20 min at 4 °C, and the supernatants were separated by SDS-PAGE and transferred onto polyvinyl difluoride (PVDF) membranes (Millipore). After being blocked with 5% nonfat milk in Tris-buffered saline (TBS) containing 0.1% Tween 20, the membranes were probed with the indicated primary antibodies. After another wash, the membranes were probed with HRP-conjugated secondary antibodies (Cell Signaling). For dot-blot analyses, cell lysates were spotted onto PVDF membranes. The membranes were blocked as described above and incubated with the indicated antibodies.

Generation and quantification of cell culture HCV RNA and infectious titer

The HCV strain JFH-1 was a gift from Dr. T. Wakita (National Institute of Infectious Diseases, Japan) (Wakita et al., 2005). Cell-culture-derived, infectious HCV was generated as described previously (Wakita et al., 2005). The HCV was quantified as follows: RNA was extracted from the Huh7 culture supernatant using the QIAamp Viral RNA Kit (Qiagen, Valencia, CA). The HCV RNA was quantified by real-time reverse transcription polymerase chain reaction using TaqMan EZ RT-PCR Core Reagents (Applied Biosystems, Foster City, CA), according to the manufacturer's protocol, using the published primers and probe (Takeuchi et al., 1999). The filtered (0.45 μm) culture supernatant of HCV-infected Huh-7.5.1 cells containing 2×10^8 HCV RNA copies/ml (equivalent to 9.7×10^4 focus-forming units [ffu]/ml) was used for experiments. To analyze HCV-RNA in the supernatant, Huh7 cells (2×10^5 cells in 6-well plate) were infected with JFH-1 (multiplicity of infection, MOI = 0.01), washed with PBS twice after 4 h, the supernatants were collected, and the cells were reseeded at 2×10^5 cells per 6-well plate at the indicated times. Huh7 cells were irradiated with X-rays (25 Gy) before infection to exclude the effect of cell proliferation in some experiments. To quantify the intracellular HCV titer, infected Huh7 cells were harvested at the indicated times and lysed by three freeze-thaw cycles. The virus titer was determined by focus-forming unit assay, as previously described (Kato et al., 2006).

Antibodies for immunoelectron microscopy

An anti-HCV-core mouse monoclonal antibody (mAb) (2H9, a gift from Dr. Wakita, National Institute of Infectious Diseases, Japan) and a human anti-E2 mAb (CBH5, a gift from Dr. Foung, Department of Pathology, Stanford School of Medicine) were used as primary antibodies. As secondary antibodies for immunoelectron microscopy, 5-nm-colloidal-immunogold-labeled anti-mouse goat IgG and 5-nm-immunogold-labeled anti-human goat IgG antibodies (EY Laboratories, San Mateo, CA) were used.

Quantitative real-time polymerase chain reaction

To confirm the knock-down of Rab27a, quantitative real-time PCR was performed. Total RNA was prepared from cells with the RNeasy Mini kit (Qiagen). Complementary deoxyribonucleic acid (cDNA) was synthesized using an oligo d(T)12–18 primer with a Primescript reverse transcriptase (Takara Bio Inc, Japan) and subjected to quantitative real-

secretion of dendritic cells is regulated by Hrs, an ESCRT-0 protein. Biochem. Biophys. Res. Commun. 399, 384–390.
Tanaka, Y., Tanaka, N., Saeki, Y., Tanaka, K., Murakami, M., Hirano, T., Ishii, N., Sugamura, K., 2008. c-Cbl-dependent monoubiquitination and lysosomal degradation of gp130. Mol. Cell. Biol. 28, 4805–4818.
Tanida, I., Fukasawa, M., Ueno, T., Kominami, E., Wakita, T., Hanada, K., 2009. Knockdown of autophagy-related gene decreases the production of infectious hepatitis C virus particles. Autophagy 5, 937–945.
van Niel, G., Porto-Carreiro, I., Simoes, S., Raposo, G., 2006. Exosomes: a common pathway for a specialized function. J. Biochem. 140, 13–21.
Wakita, T., Pietschmann, T., Kato, T., Date, T., Miyamoto, M., Zhao, Z., Murthy, K., Habermann, A., Krausslich, H.G., Mizokami, M., Bartenschlager, R., Liang, T.J., 2005. Production of infectious hepatitis C virus in tissue culture from a cloned viral genome. Nat. Med. 11, 791–796.
Wollert, T., Hurley, J.H., 2010. Molecular mechanism of multivesicular body biogenesis by ESCRT complexes. Nature 464, 864–869.

OPEN ACCESS Freely available online

PLOS | ONE

CD271 Defines a Stem Cell-Like Population in Hypopharyngeal Cancer

Takayuki Imai[1,4,6], Keiichi Tamai[1,6], Sayuri Oizumi[1], Kyoko Oyama[1], Kazunori Yamaguchi[2,6], Ikuro Sato[5], Kennichi Satoh[3], Kazuto Matsuura[4], Shigeru Saijo[4], Kazuo Sugamura[2], Nobuyuki Tanaka[1,6]*

1 Division of Cancer Biology and Therapeutics, Miyagi Cancer Center Research Institute, Natori, Miyagi, Japan, **2** Molecular and Cellular Oncology, Miyagi Cancer Center Research Institute, Natori, Miyagi, Japan, **3** Cancer Stem Cell, Miyagi Cancer Center Research Institute, Natori, Miyagi, Japan, **4** Department of Head and Neck Surgery, Miyagi Cancer Center, Natori, Miyagi, Japan, **5** Department of Pathology, Miyagi Cancer Center, Natori, Miyagi, Japan, **6** Cancer Pathology, Department of Cancer Science, Tohoku University Graduate School of Medicine, Sendai, Miyagi, Japan

Abstract

Cancer stem cells contribute to the malignant phenotypes of a variety of cancers, but markers to identify human hypopharyngeal cancer (HPC) stem cells remain poorly understood. Here, we report that the $CD271^+$ population sorted from xenotransplanted HPCs possesses an enhanced tumor-initiating capability in immunodeficient mice. Tumors generated from the $CD271^+$ cells contained both $CD271^+$ and $CD271^-$ cells, indicating that the population could undergo differentiation. Immunohistological analyses of the tumors revealed that the $CD271^+$ cells localized to a perivascular niche near $CD34^+$ vasculature, to invasive fronts, and to the basal layer. In accordance with these characteristics, a stemness marker, *Nanog*, and *matrix metalloproteinases (MMPs)*, which are implicated in cancer invasion, were significantly up-regulated in the $CD271^+$ compared to the $CD271^-$ cell population. Furthermore, using primary HPC specimens, we demonstrated that high CD271 expression was correlated with a poor prognosis for patients. Taken together, our findings indicate that CD271 is a novel marker for HPC stem-like cells and for HPC prognosis.

Citation: Imai T, Tamai K, Oizumi S, Oyama K, Yamaguchi K, et al. (2013) CD271 Defines a Stem Cell-Like Population in Hypopharyngeal Cancer. PLoS ONE 8(4): e62002. doi:10.1371/journal.pone.0062002

Editor: Vladimir V. Kalinichenko, Cincinnati Children's Hospital Medical Center, United States of America

Received December 12, 2012; **Accepted** March 17, 2013; **Published** April 23, 2013

Copyright: © 2013 Imai et al. This is an open-access article distributed under the terms of the Creative Commons Attribution License, which permits unrestricted use, distribution, and reproduction in any medium, provided the original author and source are credited.

Funding: This work was supported by JSPS KAKENHI grant numbers 24300326, 21791589, 24592613, JST CREST, and grants-in-aid from the Ministry of Health, Labour and Welfare, and Takeda Medical foundation, the Ichiro Kanehara foundation. The funders had no role in study design, data collection and analysis, decision to publish, or preparation of the manuscript.

Competing Interests: The authors have declared that no competing interests exist.

* E-mail: tanaka@med.tohoku.ac.jp

Introduction

Head and neck squamous cell carcinoma (HNSCC) is the sixth most common cancer worldwide, with nearly 500,000 new cases and an estimated 300,000 deaths reported every year. This term includes various independent cancers, such as oral, nasopharyngeal, oropharyngeal, and hypopharyngeal cancers [1]. Hypopharyngeal cancer (HPC), a malignancy of the hypopharynx, accounts for approximately 10% of all HNSCCs. Epidemiological studies indicate that tobacco and alcohol consumption contribute to its carcinogenesis [2]. Unfortunately, about 80% of HPC cases are advanced at the time of diagnosis, i.e., the patients are in stage III or IV [3], so treatment is difficult. Radical surgery such as total laryngopharyngoesophagectomy results in loss of the voice, and concurrent chemoradiotherapy often causes life-threatening side effects. Delayed regional lymph node metastasis, distant metastasis, and additional primary malignancies frequently occur during the course of the disease [3]. The 5-year survival rate of HPC patients is no more than 30% [4], suggesting a strong need for innovative treatment strategies.

The accumulating evidence of recent years supports the cancer stem cell (or initiating cell) theory [5,6]. In this fascinating scenario, cancers are composed of a hierarchy of heterogeneous cell populations, and are initiated from a limited subpopulation of cells with stem cell-like properties. With their self-renewal activity and tumor-initiating capability, cancer stem cells (CSCs) or cancer initiating cells (CICs) generate non-cancer stem cells as an 'Offspring' population. Resistance to chemotherapy and radiotherapy is another characteristic of CSCs. Thus, CSCs can be responsible for treatment failures of chemotherapy and radiotherapy, and poor clinical outcomes. Toward the goal of developing new CSC-targeting therapies, researchers have sought to identify and characterize cell-surface markers for CSCs.

In HNSCC, $CD44^+$ cells have been identified as CSCs. When clinical cancer specimens are xenografted into immunodeficient mice, $CD44^+$ cells but not $CD44^-$ cells initiate tumors, and the resulting tumors generate a hierarchy of heterogeneous cell populations [7]. However, a recent study showed that $CD44^-$ cells form spheres, possess tumor-initiating capability, and are chemoresistant, like $CD44^+$ cells [8]. Thus, the CSCs may be dynamic and heterogeneous in various microenvironments [9], and the $CD44^+$ cells may not represent pure HNSCC CSCs. In addition, HNSCC itself is heterogeneous, representing various cancer types, as described above. Therefore, targeting research for each cancer type may lead to the identification of additional CSC markers.

CD271 is a transmembrane protein that belongs to the tumor necrosis factor receptor superfamily. It is also a nerve growth factor receptor (NGFR), and interacts with neurotrophins, such as NGF, brain-derived neurotrophic factor (BDNF), neurotrophin-3 (NT3), and neurotrophin-4 (NT4), with low affinity [10]. Former

studies suggest that the tissue stem cells of oral [11], laryngeal [12], and esophageal [13] squamous epithelia express CD271. CD271 is also associated with the CSCs of malignant melanoma [14,15] and esophageal squamous cell carcinoma [16].

In the present study, we demonstrate that the $CD271^+$ cell population of HPC possesses tumor-initiating capability *in vivo*, and has several CSC-like characteristics.

Materials and Methods

Tumor Implantation

After obtaining informed consent, fresh tumor specimens were obtained at the Miyagi Cancer Center (MCC), transported to the laboratory in cooled PBS(−), and subjected to further analyses. All tumor samples were anonymized in accordance with the MCC Institutional Review Board. NOD/SCID/IL-2RγC^{null} (NOG) mice purchased from the Central Institute for Experimental Animals Japan were anesthetized with pentobarbital. Once the mice were asleep, skin incisions were made, and small pieces of tumor specimens about 50 mm^3 were implanted under the skin of the flank on both sides. Tumor formation was monitored weekly, and the tumor volume was calculated by the formula: 1/2×vertical range×horizontal range×height. When the original tumors in the xenotransplanted NOG mice reached over 10 mm in diameter, the mice were sacrificed, and the tumors were divided into samples for single-cell digestion, sphere formation, formalin fixation for histology, or serial passage in mice. The animal care and experimental protocols were performed in strict accordance with the procedures and guidelines established by the MCC administrative panels for laboratory animal care. All surgeries were performed under anesthesia, and all efforts were made to minimize suffering.

Preparation of Single-cell Suspensions from Tumor Tissue Specimens

Under aseptic conditions, tumors were cut into small fragments, and finely minced with a sterile scalpel. After being washed with PBS(−), the tumor tissue was soaked in a solution containing PBS(−), 1 mg/ml DNaseI (Roche), and 1 mg/ml Collagenase/Dispase (Roche), and incubated at 37°C for 2 or 3 hours, until complete digestion had occurred. The cells were passed through a 40-μm nylon mesh, and washed 3 times with PBS(−). After centrifugation, the pool of single cells was divided, and the cells were used for FACS analyses or sphere culture. For sphere culture, the cells were suspended in serum-free DMEM/F12 supplemented with B27 (Invitrogen), human recombinant epidermal growth factor (EGF: 20 ng/μl: Peprotech), and human basic fibroblast growth factor (bFGF: 20 ng/μl: Peprotech) on ultra-low attachment culture dishes (Corning).

Flow Cytometry Analysis and Cell Sorting

Dissociated single cells were suspended in PBS(-) with 3% FBS. The cells were stained with anti-human specific EpCAM antibodies (1:10, FITC-conjugated, Miltenyi Biotec), anti-human CD271 antibodies (1:10, APC-conjugated, Miltenyi Biotec), anti-human CD44 antibodies (1:10, APC-conjugated, Becton Dickinson), anti-human CD133 antibodies (1:10, APC-conjugated, Miltenyi Biotec), and anti-mouse IgG1, κ isotype control antibodies (1:20, APC and FITC-conjugated, Biolegend and Becton Dickinson, respectively). 7-AAD was used to exclude dead cells (Sigma, 1 μg/ml). The stained cells were either analyzed with a FACSCanto™ II (Becton Dickinson) or sorted with a FACSAria™ II (Becton Dickinson), in accordance with the manufacturer's protocol.

Real-time Reverse Transcription (RT)-PCR

The total RNA was purified from sorted single cells or tissue specimens using a mirVana™ miRNA Isolation Kit (Ambion), and transcribed using a PrimScript II cDNA Synthesis Kit (Takara Bio). Real-time RT-PCR was performed using Brilliant III Ultra-Fast SYBR Green QPCR Master Mix (Agilent Technologies). *GAPDH* was used as an endogenous reference gene. The primer sequences used for real-time RT-PCR are listed in **Table S1**.

Immunohistochemistry (IHC)

Paraffin-embedded, formalin-fixed, 3-μm tissue sections were deparaffinized in xylene, and rehydrated through ethanol to distilled water. Heat-induced epitope retrieval was performed by microwaving sections in a pH 9.0 target retrieval solution (Dako). The endogenous peroxidase was blocked with 0.3% H_2O_2. The sections were incubated with primary antibodies to human CD271 (1:4000, BD Biosciences) for 20 min, or to CD34 (Nichirei Biosciences) or Ki-67 (1:10, Santa Cruz Biotechnology) for 60 min, at 37°C. The sections stained for CD271 were incubated for 15 min with mouse LINKER (Dako), then secondary antibodies and DAB Chromogen (Envision™ FLEX Kit, Dako) were applied as described in the manufacturer's protocol. To the sections stained for CD34 or Ki-67, Simple Stain AP (M) (Nichirei Biosciences) was applied as the secondary antibody, and the staining was visualized with New Fuchsin Substrate (Nichirei Biosciences). For the double staining of CD34 or Ki-67,with CD271, the CD34 or Ki-67 staining was performed first, followed by that for CD271, as described above.

In vivo Tumorigenesis Assay

Dissociated tumors were sorted based on the human EpCAM and CD271 expression, as $EpCAM^+$ $CD271^+$ cells or $EpCAM^+$ $CD271^-$ cells. The sorted cells were suspended in 200 μl of Matrigel matrix (BD Biosciences) at 4°C, then subcutaneously injected into the flanks of NOG mice with a 1-ml syringe. Each mouse received $CD271^+$ cells in the right side, and $CD271^-$ cells in the left. Tumor formation was monitored by weekly inspection and palpation.

In vivo Chemotherapy Assay

Cisplatin (CDDP), an anti-cancer drug classified as a platinum reagent, was administered intravenously or intraperitoneally at 5 or 7.5 mg/kg. One week later, the mice were euthanized, and the tumors were extracted. The tumors were divided and either fixed with formalin for IHC, or dissociated into single cells and subjected to FACS analysis.

Statistics

The analyses of disease-specific survival and relapse-free survival were conducted with Kaplan-Meier methods, and the log rank test was used to evaluate the difference between groups. Fisher's exact test was used to compare two groups ("strong" versus "moderate-to-weak" CD271 expression) in resected tumors from 28 cases of HPC, and the chi-square test was used to compare the same two groups in the IHC study of 83 HPC cases. The average values of *Nanog* expression between the two groups was analyzed with Student's t-test. The level of significance was set at $p<0.05$.

Ethics

The Institutional Review Board of the MCC approved this study protocol, and written informed consent was obtained from each subject. The protocol of animal experiments was approved

by the MCC Animal Care and Use Committee (Permit Number: MCC-AE-2011-8).

Results

HPC Tumors Include a Subpopulation of CD271$^+$ Cells

To investigate tumor initiation and cancer stem cells, fresh primary tumor specimens obtained from HPC patients undergoing surgery were implanted under the skin of 8-10-week-old NOG mice. Three independent human HPC specimens with similar clinical characteristics were used to establish primary xenograft lines (HPCM1-3) (**Table S2**). The histology of each xenograft was consistent with its primary sample (**Figure S1**).

To characterize the serially xenotransplanted tumor lines, their cell-surface marker expression was analyzed. Each tumor was extracted from the host and prepared as a single-cell suspension. Because EpCAM is reported to be a diagnostic tumor-cell marker for HNSCC [17], the human EpCAM-positive cells were strictly gated to eliminate host-derived cells, and analyzed by flow cytometry. Among the CSC markers tested, the cells were negative for CD133, and 3.4% of the tumor cells were positive for CD44 (data not shown). Unexpectedly, we observed a CD271$^+$ subpopulation among the three HPC lines tested (**Figure 1A**). In repeated experiments, the CD271$^+$ population represented 2.99 to 20.1% of the cells in HPCM1. Similar CD271$^+$ populations were clearly present in the other two lines: 2.90–9.54% for HPCM2 and 19.1% for HPCM3. Next, we analyzed paraffin-embedded sections of tumors derived from the xenotransplanted HPC lines for CD271 by IHC (**Figure 1B**). Within the typical squamous cell carcinomas formed by the three lines, CD271$^+$ cells were mainly present in the basal layer of the tumor, almost restricted to the peripheral zone of the tumor nest, and scarce in the center portion (**Figure 1B**). Under high magnification, CD271$^+$ cells were observed next to the stroma (**Figure 1B–d**). These CD271$^+$ cells exhibited morphologically immature phenotypes, whereas the CD271$^-$ cells in the central zone of the tumor nest had more mature, flattened, and keratinized shapes (**Figure 1B–e**). To further characterize the localization of CD271$^+$ cells within the HPC, we stained cytokeratins (CKs) in serial sections (**Figure S2**). CK5/6 tends to localize to basal layers and proliferating suprabasal compartments, and the CD271$^+$ cells were localized within the CK5/6-positive region. The CD271$^+$ cells were also moderately positive for CK8, which marks undifferentiated SCC cells. These results suggest that the CD271$^+$ population is included in the basal-layer portion of the CK5/6-positive area, and partially overlaps with CK8-positive undifferentiated cells.

We also examined the CD271 expression within clinically dissected HPC specimens. First, we confirmed that CD271$^+$ cells were present in the most basal layer of normal hypopharyngeal mucosa (**Figure 1C–a**). Similarly, in a carcinoma *in situ* (*CIS*) specimen, CD271$^+$ cells were restricted to the basal layer, and were absent from the more differentiated upper layers (**Figure 1C–b**). Typically, most of the cancer cells located in the invasive front were CD271$^+$ (**Figure 1C–c,d**). We also examined whether CD271$^+$ cells were located close to the vasculature within tumors. We found that CD34$^+$ microvascular endothelial cells (red in **Figure 1D**) were located in the CD271$^+$ cell areas, and magnified images showed that some CD34$^+$ and CD271$^+$ cells were near each other, or in direct contact (**Figure 1D–a,b**). Of note, in most of the specimens, the CD271$^+$ cells formed dense clusters that were surrounded by stroma, which contained CD34$^+$ microvessels (**Figure 1D–c,d,e**). Together, these data indicated that CD271$^+$ cells are present in the invasive front and in the perivascular area of tumors.It is well known that cells from various cancers, including HNSCC, that form spheres under suspension culture conditions include CSCs [18]. Hence, we examined whether sphere-formation culture would affect the CD271 expression. Dissociated cancer cells generated spheres that survived for 12 days, and single cells prepared from these spheres were subjected to CD271 analysis (**Figure 1E**). CD271 was expressed in 46.5% of these cells, in contrast to the original HPCM1 cell tumor, in which 2.99–20.1% of the cells were CD271$^+$. This result suggested that *in vitro* sphere formation caused the enrichment of CD271$^+$ cells.

We also examined whether the CD271$^+$ cells are a proliferating population. Double -staining experiments with Ki-67 and CD271 showed that the CD271$^+$ cells mostly resided in the basal layer, whereas the Ki-67-positive cells localized mainly to the relatively differentiated suprabasal layers (Figure 1F). These results suggest that the CD271$^+$ cells are not actively proliferating *in vivo*.

CD271$^+$ Cells are Tumorigenic and Differentiate *in vivo*

We next examined the *in vivo* tumorigenicity of the CD271$^+$ cells of the three HPC lines. Thirty to 100,000 CD271$^+$ or CD271$^-$ cells were subcutaneously injected into each side of the same mouse to avoid any host/environmental differences (**Figure 2A**). The accuracy of sorting was confirmed by FACS analysis (**Figure 2B**). The xenotransplantation results are summarized in **Table 1**. In HPCM1, the CD271$^+$ cells initiated tumors at an extremely high rate, even when fewer than 300 cells (but at least 30 cells) were injected. Thirty CD271$^-$ cells generated a tumor in only one of six inoculations, and the tumor that formed was much smaller than those initiated by the CD271$^+$ cells (**Figure 2C**). Similarly, for HPCM2, all the tumors that formed, except for one, arose from CD271$^+$ cells. Although the CD271$^-$ cells in HPCM3 generated tumors, they showed a longer latency and lower frequency than those that developed from CD271$^+$ cells. These data indicated that the CD271$^+$ cells possessed higher tumorigenicity than the CD271$^-$ cells *in vivo*.

Morphologically, the CD271$^+$ cells formed tumors that resembled the original one histologically, with typical SCC features: basal cell-like morphology in the peripheral zone, and differentiated cells in the central portion of the tumor nest (**Figure 2D**). The generated tumors were also examined for CD271 expression by flow cytometry. The tumors arising from the CD271$^+$ cells contained both CD271$^+$ and CD271$^-$ cells (**Figure 2D**). Thus, the CD271$^+$ population has the potential to generate a hierarchy of CD271-expressing and non-expressing cells, as well as the ability to initiate cancer.

Gene Expression Profile of CD271$^+$ Cells Reveals Some Characteristics of Stemness and Invasiveness

We next asked whether the CD271$^+$ population had characteristics associated with malignant cells in terms of stemness and invasion/metastasis. First, the expression of pluripotent stem cell-related genes, *Nanog*, *Sox2*, and *Oct-4* was examined. Real-time RT-PCR analyses indicated that the *Nanog* expression was significantly higher in the CD271$^+$ cells of the three HPC lines than in the CD271$^-$ cells (**Figure 3A**). IHC of serial sections showed the inclusion of CD271$^+$ cells in the Nanog-positive basal layer (**Figure S3A**). However, the expression of *Sox2* and *Oct-4* showed no consistent tendency (**Figure S4**). Next, the expression of three secretion-type invasion-related genes, *MMP1*, *MMP2*, and *MMP10* was examined (**Figure 3B**). CD271$^+$ cells from the three HPC lines showed a marked elevation in *MMP1*, which ranged from 2.3 to 7.3-fold compared with the CD271$^-$ cells. Likewise, *MMP2* was increased 3.6–4 fold in the CD271$^+$ cells. Prominent *MMP10* up-regulation was seen in the CD271$^+$ population of

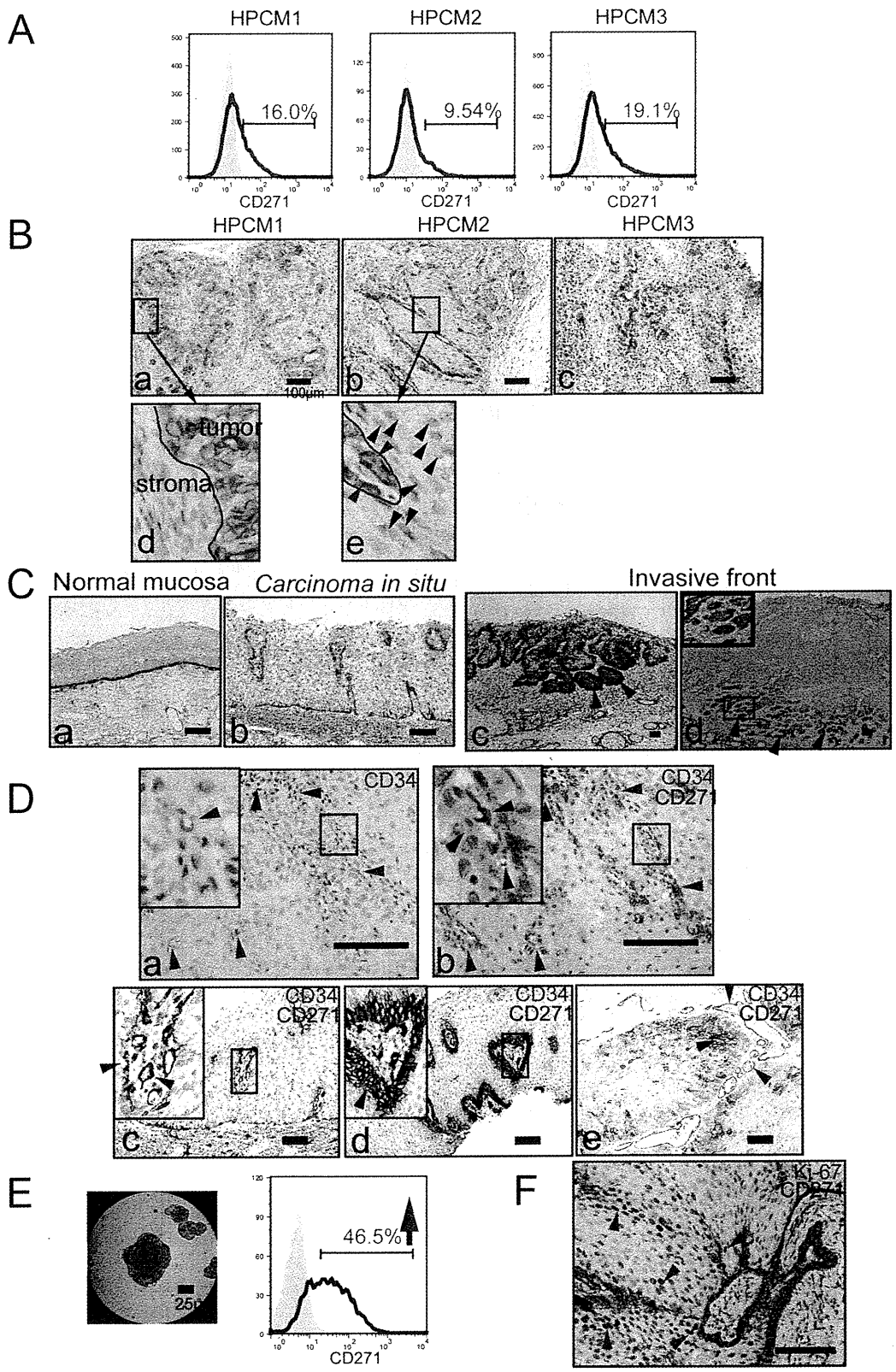
A
HPCM1
HPCM2
HPCM3
16.0%
9.54%
19.1%
CD271
B
HPCM1
HPCM2
HPCM3
a
b
c
100μm
tumor
stroma
d
e
C
Normal mucosa
Carcinoma in situ
Invasive front
a
b
c
d
D
CD34
CD34
CD271
a
b
CD34
CD271
CD34
CD271
CD34
CD271
c
d
e
E
25μ
46.5%
CD271
F
Ki-67
CD271